An artificial tetramerization domain restores efficient assembly of functional Shaker channels lacking T1

Noa Zerangue, Yuh Nung Jan, and Lily Yeh Jan*

Howard Hughes Medical Institute, Departments of Physiology and Biochemistry, Program in Neuroscience, University of California, San Francisco, CA 94143-0725

Contributed by Lily Yeh Jan, January 13, 2000

One feature shared by all Shaker-type voltage-gated K^+ channels is a highly conserved domain (T1) located in the cytoplasmic N terminus. The T1 domain is a key determinant of which subtypes can form heteromultimeric channels, suggesting that T1 functions during channel assembly. To better define the role of T1 during channel assembly and separate this function from potential contributions to channel permeation and gating, we replaced the T1 domain (residues 96–183) of ShakerB with a coiled-coil sequence (GCN4-LI) that forms parallel tetramers. Deleting T1 dramatically, but not completely, abolished channel formation under most expression conditions. Channels lacking T1 are functional and K^+-selective, although they activate at more hyperpolarized membrane potentials and inactivate less completely. Insertion of the artificial tetramerization domain (GCN4-LI) restored efficient channel formation, suggesting that tetramerization of the cytoplasmic T1 domain promotes transmembrane channel assembly by increasing the effective local subunit concentration for T1 compatible subunits. We propose that T1 tetramerization promotes subfamily-specific assembly through kinetic partitioning of the assembly process, but is not required for subsequent steps in channel assembly and folding.

The basic architecture of voltage-gated potassium channels has begun to be revealed through a convergence of structure–function studies and crystallography. A recurring theme that emerges from these studies is symmetrical tetrameric organization. The minimal voltage-gated potassium channel consists of four subunits, each containing six transmembrane segments (1, 2). The fifth and sixth transmembrane segments along with the highly conserved pore–helix and pore–loop domain form an ion-conducting pore in which each of the four subunits contribute equally to the permeation pathway (3–5). For voltage-gated potassium channels, the tetrameric architecture of the transmembrane structure is mirrored by a similar 4-fold symmetry in the tetrameric structure of the cytoplasmic N-terminal domain (T1) (6–8). Regulatory subunits also appear to share a tetrameric organization (9). These studies lead one to envision voltage-gated potassium channels built up from multiple layers of interconnected tetrameric structures.

Our understanding of the architecture of functional potassium channels reflects only the endpoint of a complex and poorly understood assembly pathway. Current research is beginning to elucidate the intermediate steps between the synthesis and insertion of individual subunits into the membrane of the endoplasmic reticulum (ER) and the final correctly assembled and folded channel (10). The N-terminal T1 domain, conserved among all voltage-gated K^+ channels, has emerged as an important component in the assembly process. The T1 domain has been shown to spontaneously form tetramers in the absence of hydrophobic transmembrane sequences (6, 7). A number of studies have shown that deletion of T1 impairs channel assembly (1, 6, 10–14). Furthermore, the T1 domain determines which subtypes of voltage-gated K^+ channels can coassemble, and T1 compatibility restricts assembly to subunits within *Shaker*, *Shab*, *Shaw*, and *Shal* subfamilies (6, 13, 15, 16). These biochemical and functional findings have been confirmed by crystal structures of tetrameric T1 domains from each subfamily (7, 8). Analysis of chimeras between members of different subfamilies of voltage-gated K^+ channels has shown that the transmembrane pore-forming domains from different subfamilies are capable of coassembly provided the T1 domains are compatible (6). These results, taken together, imply that T1 functions normally to prevent promiscuous interactions between hydrophobic transmembrane domains of subunits from different subfamilies.

The crystal structure of T1 has revealed that the T1 tetramer contains a water-filled pore along its 4-fold axis (7). This finding raises the possibility that the T1 pore could be continuous with the transmembrane pore and potentially contribute to the permeation pathway. Furthermore, because the N-terminal inactivation ball is situated at the beginning of the N terminus, close association of a tetrameric T1 structure with the membrane-spanning portion of the channel could modulate the access of the inactivation ball to its membrane-proximal gate. It is also conceivable that such close interactions could affect voltage-dependent conformational changes underlying channel activation. These possibilities have led to speculation that T1 also may participate in channel gating.

To address how T1 functions during assembly and gating, we have removed the T1 domain and replaced it with a 33-aa coiled-coil domain (GCN4-LI) that forms parallel tetramers (17). Addition of this artificial multimerization domain greatly improves the assembly efficiency of channels lacking T1. Channels lacking T1 exhibited properties similar but not identical to those of wild-type ShakerB (ShB) channels. Although the T1 domain does not appear to be required for basic channel function, the differences observed indicate that the presence of T1 may influence channel gating. We conclude that T1 promotes the channel assembly by increasing the local concentration of hydrophobic transmembrane domains belonging to subunits with compatible T1 domains.

Materials and Methods

Molecular Biology. The T1 domain (96–183) was deleted by using PCR mutagenesis and replaced with *Apa*I and *Mlu*1 sites. The final amino acid sequence was C_{96}**NASATGAQD**$_{184}$. The GCN4-LI sequence was amplified by primers containing *Apa*1 and *Mlu*1 in the 5′ and 3′ flanking regions, respectively, and inserted into ShΔ96–183. ShBΔ96–183$_{GCN4LI}$ reads C_{96}**NASARMKQIEDKLEEILSKLYHIENELARIKKLLGERT GAQD**$_{184}$. Further aspartate mutations (underlined) were introduced into ShBΔ96–183$_{GCN4LI}$, and it reads C_{96}**NASARMKQIEDKLEE<u>D</u>LSKLYH<u>D</u>ENELARIKKLLGER-**

Abbreviations: ShB, ShakerB; T1, cytoplasmic tetramerization domain; ER, endoplasmic reticulum.

*To whom reprint requests should be addressed at: Howard Hughes Medical Institute, Box 0725, University of California, San Francisco, CA 94143-0725. E-mail gkw@itsa.ucsf.edu.

The publication costs of this article were defrayed in part by page charge payment. This article must therefore be hereby marked "*advertisement*" in accordance with 18 U.S.C. §1734 solely to indicate this fact.

Article published online before print: *Proc. Natl. Acad. Sci. USA*, 10.1073/pnas.060016797. Article and publication date are at www.pnas.org/cgi/doi/10.1073/pnas.060016797

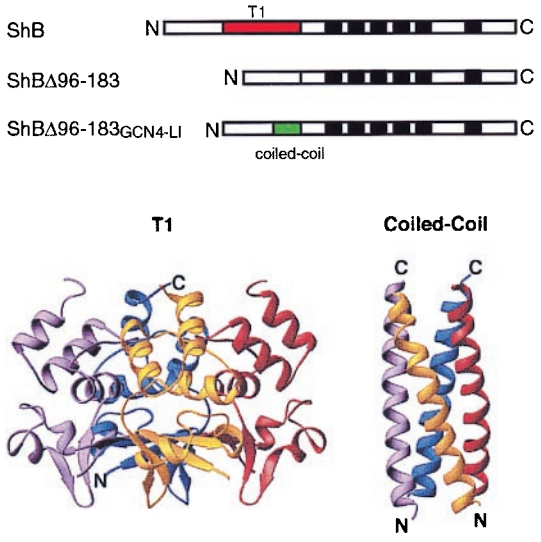

Fig. 1. (*Upper*) Schematic illustration of ShB, ShBΔ96–183, and ShBΔ96–183_{GCN4LI} constructs. (*Lower*) Crystal structures of T1 (7) and GCN4-LI (17).

$TGAQD_{184}$. All mutations introduced by PCR mutagenesis were verified by sequencing. All constructs were created in the oocyte expression plasmid pGEMHE. Polyadenylated RNA was made by T7 *in vitro* transcription (Epicentre Technologies, Madison, WI) of *Nhe*1-linearized cDNA.

Preparation and Injection of *Xenopus* Oocytes. Oocytes were removed and defolliculated by collagenase treatment as described (18). Cells were maintained at 16°C in ND96 (100 mM Na^+/2 mM K^+/1.8 mM Ca^{2+}/1 mM Mg^{2+}/10 mM Hepes, pH 7.45, with antibiotics). Oocytes were injected with 45 μl of solution containing various concentrations of RNA as indicated.

Electrophysiology. Currents were measured 1–4 days after injection by using a two-electrode voltage clamp (Dagan Amplifier; Dagan Instruments, Minneapolis; PCLAMP software). Electrodes (1 MΩ) were filled with 3 M KCl, and voltage-activated currents were isolated by leak subtraction. Unless otherwise stated, oocytes were bathed in ND96 and clamped at −80 mV, and currents were elicited by 80-ms steps to depolarizing potentials.

Results

Concentration Dependence of ShB Channels Lacking T1. Deleting the T1 domain of ShB (residues 96–183, schematized in Fig. 1) largely abolished channel formation in *Xenopus* oocytes (Fig. 2), as has been reported (10). We next varied the expression levels of ShB and ShBΔ96–183 by varying the amount of RNA injected. For ShB, voltage-dependent, fast-inactivating K^+ currents were observed within 24 h even at the lowest RNA concentration tested (0.5 ng/oocyte). However, for ShBΔ96–183, currents were observed in only three of seven batches of injected oocytes and only at the highest RNA concentration tested (10 ng) and after 72 h. This result implies that removing T1 severely impairs assembly efficiency, but increasing subunit concentration can partially overcome this assembly defect.

Because ShBΔ96–183 subunits lacking T1 could still form channels when expressed at high levels, we reasoned that T1 may function normally to enhance channel assembly by increasing the likelihood of transmembrane domains being in close proximity to one another. To test the hypothesis that tetramerization of cytoplasmic domains stimulates transmembrane assembly, we inserted an artificial tetramerization domain into the same

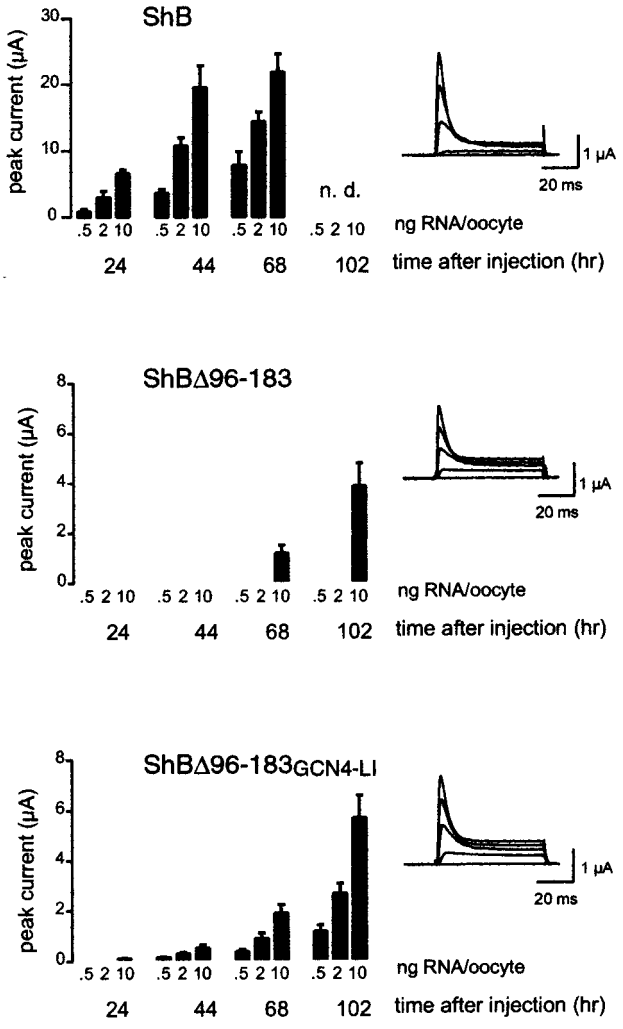

Fig. 2. Efficiency of channel formation determined by time course and RNA dose response of ShB, ShBΔ96–183, and ShBΔ96–183_{GCN4LI}. Oocytes were injected with concentrations of RNA as indicated. Peak currents resulting from a depolarization from −80 mV to + 30 mV at different times after injection are plotted in graph. Data points reflect mean and SE for 3–5 oocytes. Leak-subtracted currents from two electrode voltage-clamp recordings were elicited by 100-ms depolarizing steps from a holding potential of −80 mV to −30, −10, 10, 30, and 50 mV in 2 mM K^+.

position in ShB as T1. The artificial tetramerization domain we used was the 33-aa GCN4-LI peptide (17). We chose the GCN4-LI sequence because it has been reported to form extremely stable parallel tetrameric, but not dimeric or trimeric, coiled-coil structures. These features as well as its length along its central axis (48 Å vs. 40 Å for Shaker T1) make it a good candidate to mimic T1 tetramerization. In contrast to the inefficient formation of ShBΔ96–183 channels, channels of ShBΔ96–183_{GCN4LI} were observed at the lowest concentration of RNA (0.5 ng/oocyte) tested and after 24 h (Fig. 2). Enhanced efficiency of channel formation because of the GCN4-LI peptide was abolished by substituting aspartates for two buried isoleucines critical for tetramerization of the coiled coil (data not shown), demonstrating that interactions between coiled-coil domains are responsible for the enhanced assembly efficiency. Although insertion of the GCN4-LI peptide into ShBΔ96–183 resulted in channel formation at lower expression levels and at shorter time points after injection, it should be noted that the magnitude of ShBΔ96–183_{GCN4LI} currents were consistently less

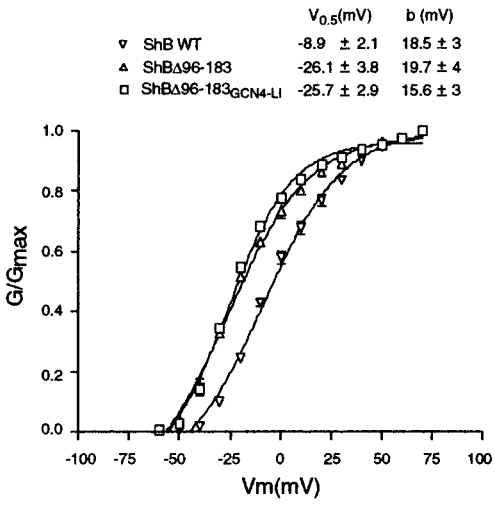

Fig. 3. Voltage-activation relationship for ShB, ShBΔ96–183, and ShBΔ96–183_{GCN4LI} channels. Conductance was calculated from peak currents elicited by depolarizations from −80 mV in 2 mM K^+. Voltage-conductance plots from 4–6 oocytes were averaged and fitted to the Boltzmann equation.

than that of wild-type ShB currents. Consistent with these observations, each of the three constructs exhibited similar protein levels on Western blots, but only ShB showed a high percentage of mature glycosylated protein (data not shown).

To determine whether T1 contributes to the functioning of fully assembled channels, we next characterized the properties of channels lacking T1. Both ShBΔ96–183 and ShBΔ96–183_{GCN4LI} were K^+-selective as determined by reversal potentials of tail currents in 30 mM K^+ (−34 ± 1 mV and −37 ± 3 mV, respectively) and 90 mM K^+ (−6 ± 2 mV and −8 ± 1 mV, respectively). The reversal potentials obtained for channels lacking T1 were similar to ShB and consistent with high K^+ selectivity. Although both ShBΔ96–183 and ShBΔ96–183_{GCN4LI} were activated by depolarizing pulses, the voltage dependence of activation was shifted approximately 15 mV more negative in channels lacking T1 (Fig. 3). The slope of voltage activation was not significantly different between the constructs tested (Fig. 3). Furthermore, channels lacking T1 also exhibited fast inactivation (Fig. 2) with rates similar to wild-type ShB channels. However, channels lacking T1 exhibited less complete fast inactivation (Fig. 2). In oocytes expressing 1- to 2-μA peak current during pulses to +60 mV, ShB channels inactivated 92 ± 4% after 60 ms, whereas ShBΔ96–183 and ShBΔ96–183_{GCN4LI} inactivated only 74 ± 7% and 67 ± 5%, respectively.

Discussion

In this study we addressed the function of Shaker T1 by analyzing channel formation in ShB subunits lacking T1 and by functionally replacing T1 with an unrelated artificial tetramerization domain (Fig. 1). We find that ShB subunits lacking T1 still form functional channels, although the efficiency of channel assembly is severely impaired as assayed by current amplitude resulting from injections of different concentrations of RNA and at different time points (Fig. 2). One previous study (10) did not observe currents from Shaker channels lacking T1 (Δ97–196), whereas another recent study (19) reported currents from Shaker channels lacking the entire N terminus (Δ1–193). This difference could arise from a negative effect of the first part of the N terminus on assembly. However, that we observe currents from ShBΔ96–183 suggests that the first 96 aa do not completely prevent channel formation in the absence of T1.

Previous studies of Kv1.3 and Kv1.4 as well as Shaker (1, 19–22) have shown that T1 is not essential for channel formation. Therefore, the transmembrane pore must be able to form in the absence of T1, and domains other than T1 must possess the capacity for subunit–subunit interactions. In addition to the permeation pathway (4), other regions such as S1 (23) and S1-S2-S3 (20, 21) have been suggested to be involved in these subunit–subunit interactions.

If T1 is not essential and other interaction domains exist in voltage-gated K^+ channels, why then does deleting T1 have such a profound but partial effect on channel assembly? Two general possibilities exist to explain these findings. First, transmembrane domains could tetramerize rapidly and efficiently without T1, but a critical membrane-folding step may require a chaperone-like function of T1. Alternatively, T1 could initiate assembly and provide the initial tetramerization event, which would be required to bring the transmembrane domains into close enough proximity for assembly. Several findings suggest that the transmembrane domains do not readily form tetramers in the absence of T1. Voltage-gated K^+ channel subunits lacking T1 do not readily form tetramers as determined by coprecipitation, cross-linking, or dominant negative studies, implying that the majority of subunits without T1 remain monomers (6, 10–12, 22). Furthermore, if ShBΔ96–183 readily formed tetramers, but inefficiently matured into functional channels, one would predict that the ratio of ShB to ShBΔ96–183 channels should be the same at all concentrations of RNA injected because the rate of folding maturation of the tetramers should not be concentration-dependent. However, ShBΔ96–183 currents were observed only at the highest concentration of RNA tested, and at all other concentrations no currents were detected (Fig. 2). This result suggests that formation of ShBΔ96–183 channels highly depends on the concentration of subunits available for assembly and that channel assembly has a threshold concentration that is greater than the subunit concentration that is normally present in most expression situations.

Our finding that either T1 or the GCN4-LI peptide greatly enhances the efficiency of channel assembly demonstrates that tetramerization of cytoplasmic domains *per se* can facilitate channel assembly. Because GCN4-LI is structurally unrelated to T1 it is unlikely that it can directly assist in the assembly and folding of the transmembrane domains. Therefore, the effect observed on channel formation must be caused by increasing the local concentration of subunits. Although the GCN4-LI peptide resulted in channel formation at lower concentrations of RNA and at earlier time points, it should be noted that current amplitude was less than that of ShB (Fig. 2). Although this result could reflect poor trafficking or reduced functionality of channels containing the GCN4-LI peptide, this difference is also consistent with a role for T1 in directly coordinating or scaffolding the folding of the transmembrane domains.

The observation that tetramerization of cytoplasmic domains is sufficient to promote channel assembly has implications for understanding how T1 functions to determine assembly compatibility. A number of studies provide compelling evidence that T1 compatibility largely determines subunit compatibility (6, 11, 13). It has been observed that T1 chimeras can coassemble with channel subunits with compatible T1 domains, thereby forming heteromultimeric pores containing subunits from different subfamilies that would not normally coassemble (16). If channels also can form in the absence of T1, how then does T1 prevent promiscuous coassembly between subunits from different subfamilies of voltage-gated K^+ channels? Based on our finding that T1 enhances assembly through facilitation of concentration-dependent transmembrane assembly, we propose that assembly is a multistep process in which rapid T1 assembly occurs first and brings the transmembrane domains of T1-compatible subunits into close proximity. The high concentration of subunits from

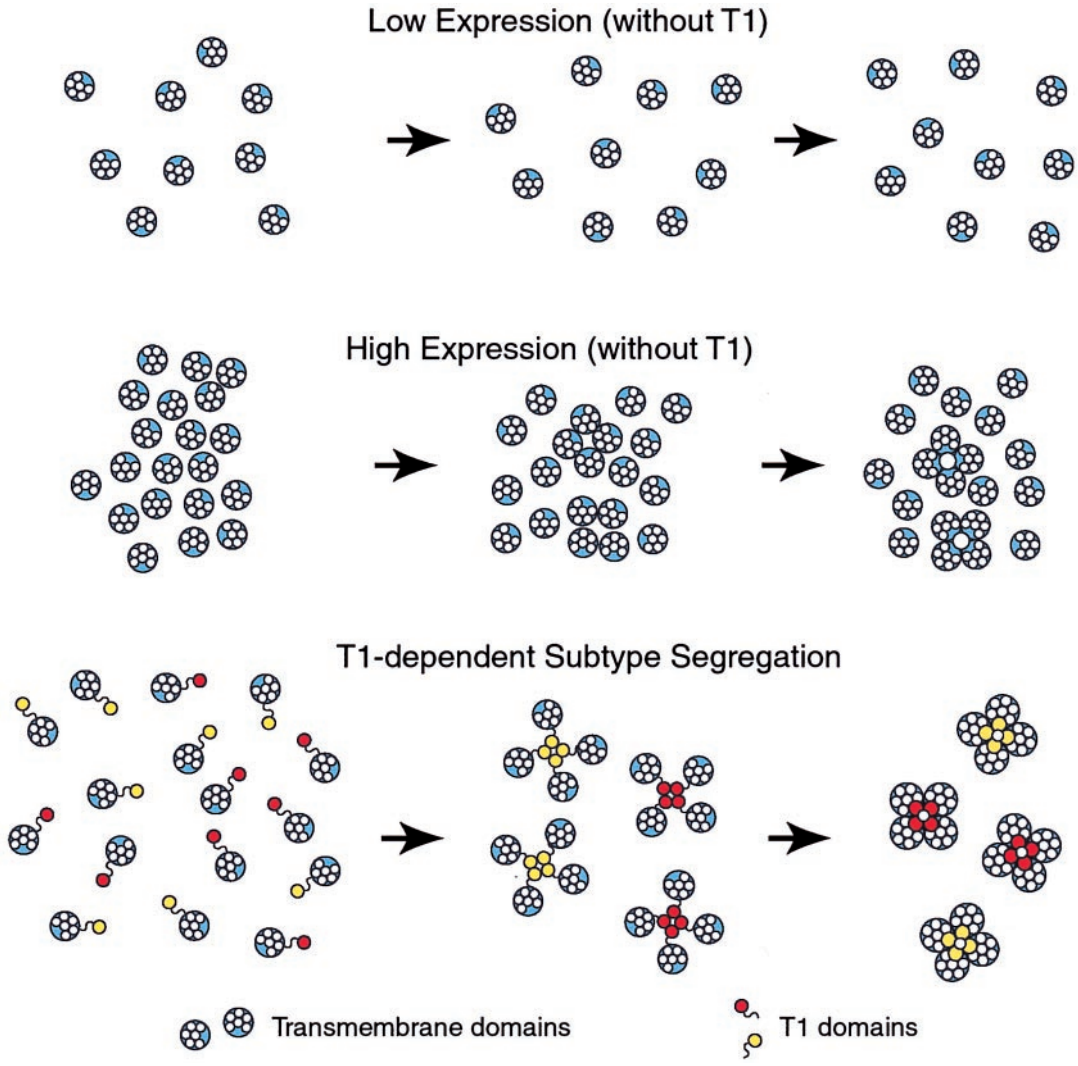

Fig. 4. Model of T1 function during voltage-gated K^+ channel assembly. (*Top*) After translation and insertion of subunits into the ER membrane, interactions between cytoplasmic T1 domains rapidly bring four monomeric subunits together, followed by slower multimerization and folding of transmembrane domains. When multiple K^+ channel subtypes are present in the ER membrane, rapid tetramerization of T1 creates a high local concentration of transmembrane subunits that favors assembly of transmembrane domains from subunits containing compatible T1 domains. (*Middle*) The transmembrane domains of ShB channels lacking T1 do not assemble into channel tetramers when subunits are present in the ER at low concentrations (*Top*). Expression conditions resulting in very high concentrations of subunits lacking T1 is sufficient for some channel assembly.

the clustering effect of T1 allows the tetramerization, assembly, and folding of the transmembrane domains. The combined effect of rapid inclusion into tetramers with compatible subunits resulting from T1 interactions and weak interactions between transmembrane domains of monomers will ensure assembly within subfamilies (Fig. 4 *Bottom*). Thus, T1 does not necessarily physically prevent promiscuous assembly, but rather subtype segregation arises from the effects of T1 on assembly kinetics. Levels of expression that typically would give large current for subunits containing T1 are insufficient for the assembly of channels lacking T1 (Fig. 4 *Top*). However, higher concentrations can partially overcome this assembly defect (Fig. 4 *Middle*). Under normal expression conditions *in vivo*, the subunit concentration in the ER is likely to be considerably lower than in heterologous overexpression situations. In such conditions, tetramerization by T1 is likely to be even more critical for efficient channel assembly and will ensure only assembly between subunits with compatible T1 domains.

Another important dimension of voltage-gated K^+ channel assembly is interaction with auxiliary subunits. Proteins such as Hyperkinetic, Kvβ1/2, src, and RhoA have been shown to interact with voltage-gated K^+ channels and alter their biogenesis and gating properties (24–26). It is interesting to note that Kvβ2, like the T1 domain, spontaneously assembles into tetramers (9) and has been shown to enhance the assembly of voltage-gated K^+ channels (24). These findings raise the possibility that Kvβ could pre-exist as a tetramer and nucleate or scaffold the tetramerization of T1 and/or the hydrophobic transmembrane domains. In such a scenario, tetramerization of T1, Kvβ, and the transmembrane domains may be interconnected during channel folding and assembly, with initial tetramerization of one domain assisting in the multimerization of another tetrameric domain. Further experiments will be required to determine how Kvβ contributes to the assembly and folding pathway of voltage-gated K^+ channels.

The observation that ShB channels lacking T1 are K^+-selective, voltage-activated, and rapidly inactivating implies that T1 is not required for assembly and folding of channels that exhibit the basic properties typical of Shaker-type K^+ channels. However, several differences were observed. Most notably, the

voltage dependence of activation was shifted 15 mV more negative for ShBΔ96–183 and ShBΔ96–183$_{GCN4LI}$ compared with wild-type ShB. This quantitative difference could reflect a role for T1 in gating conformation changes or a requirement for T1 in maintaining the normal architecture of the transmembrane domains. Furthermore, the presence of fast inactivation in channels lacking T1 suggests that T1 is not required to mediate interactions between the inactivation ball and its receptor. Also, the structurally unrelated GCN4-LI coiled coil did not impede inactivation, although fast inactivation was less complete in ShBΔ96–183 and ShBΔ96–183$_{GCN4LI}$ relative to ShB. Similar effects on voltage gating and N-type inactivation also were observed in a recent analysis of Shaker channels lacking T1 (19).

Replacing interaction domains with coiled coils that exhibit defined multimerization properties may be a generally useful strategy for uncoupling the assembly and functional contributions of interacting domains in multimeric proteins. Using dimeric and trimeric coiled-coil sequences also could provide a tool for testing intermediate steps in the assembly process.

We thank members of the Jan lab for useful discussions and Dan Minor for the GCN4-LI cDNA and image of T1 structure. This work is supported by National Institutes of Health Grant NS15963. N.Z. is the recipient of a Howard Hughes Predoctoral Fellowship. L.Y.J. and Y.N.J. are Howard Hughes Investigators.

1. Van Dongen, A. M., Frech, G. C., Drewe, J. A., Joho, R. H. & Brown, A. M. (1990) *Neuron* **4,** 433–443.
2. Shih, T. M. & Goldin, A. L. (1997) *J. Cell Biol.* **136,** 1037–1045.
3. MacKinnon, R. (1991) *Nature (London)* **350,** 232–235.
4. Doyle, D. A., Cabral, J. M., Pfuetzner, R. A., Kuo, A., Gulbis, J. M., Cohen, S. L., Chait, B. T. & MacKinnon, R. (1998) *Science* **280,** 69–76.
5. MacKinnon, R., Cohen, S. L., Kuo, A., Lee, A. & Chait, B. T. (1998) *Science* **280,** 106–109.
6. Li, M., Jan, Y. N. & Jan, L. Y. (1992) *Science* **257,** 1225–1230.
7. Kreusch, A., Pfaffinger, P. J., Stevens, C. F. & Choe, S. (1998) *Nature (London)* **392,** 945–948.
8. Bixby, K. A., Nanao, M. H., Shen, N. V., Kreusch, A., Bellamy, H., Pfaffinger, P. J. & Choe, S. (1999) *Nat. Struct. Biol.* **6,** 38–43.
9. Gulbis, J. M., Mann, S. & MacKinnon, R. (1999) *Cell* **97,** 943–952.
10. Schulteis, C. T., Nagaya, N. & Papazian, D. M. (1998) *J. Biol. Chem.* **273,** 26210–26217.
11. Shen, N. V., Chen, X., Boyer, M. M. & Pfaffinger, P. J. (1993) *Neuron* **11,** 67–76.
12. Hopkins, W. F., Demas, V. & Tempel, B. L. (1994) *J. Neurosci.* **14,** 1385–1393.
13. Covarrubias, M., Wei, A. & Salkoff, L. (1991) *Neuron* **7,** 763–773.
14. Deal, K. K., Lovinger, D. M. & Tamkun, M. M. (1994) *J. Neurosci.* **14,** 1666–1676.
15. Xu, J., Yu, W., Jan, Y. N., Jan, L. Y. & Li, M. (1995) *J. Biol. Chem.* **270,** 24761–24768.
16. Shen, N. V. & Pfaffinger, P. J. (1995) *Neuron* **14,** 625–633.
17. Harbury, P. B., Zhang, T., Kim, P. S. & Alber, T. (1993) *Science* **262,** 1401–1407.
18. Collins, A., Chuang, H., Jan, Y. N. & Jan, L. Y. (1997) *Proc. Natl. Acad. Sci. USA* **94,** 5456–5460.
19. Kobertz, W. R. & Miller, C. (1999) *Nat. Struct. Biol.* **6,** 1122–1125.
20. Tu, L. W., Santarelli, V., Sheng, Z., Skatch, W., Pain, D. & Deutsch, C. (1996) *J. Biol. Chem.* **271,** 18904–18911.
21. Sheng, Z. F., Skach, W., Santarelli, V. & Deutsch, C. (1997) *Biochemistry* **36,** 15501–15513.
22. Lee, T. E., Philipson, L. H., Kuznetsov, A. & Nelson, D. J. (1994) *Biophys. J.* **66,** 667–673.
23. Babila, T., Muscucci, A., Wang, H., Weaver, F. E. & Koren, G. (1994) *Neuron* **12,** 615–626.
24. Shi, G., Nakahira, K., Hammond, S., Rhodes, K. J., Schechter, L. E. & Trimmer, J. S. (1996) *Neuron* **16,** 843–852.
25. Holmes, T. C., Fadool, D. A., Ren, R. & Levitan, I. B. (1996) *Science* **274,** 2089–2091.
26. Cachero, T. G., Morielli, A. D. & Peralta, E. G. (1998) *Cell* **93,** 1077–1085.